Long non-coding RNA FOXD2-AS1/miR-150-5p/PFN2 axis regulates breast cancer malignancy and tumorigenesis

MING JIANG*, NI QIU*, HAOMING XIA*, HONGLING LIANG, HONGSHENG LI and XIANG AO

Department of Breast Surgery, Affiliated Cancer Hospital and Institute of Guangzhou Medical University, Guangzhou, Guangdong 510095, P.R. China

Received August 6, 2018; Accepted October 29, 2018

DOI: 10.3892/ijo.2019.4671

Abstract. Breast cancer (BC) is a common cancer and leading cause of cancer-associated mortality in women. Abnormal expression of long non-coding RNA FOXD2 adjacent opposite strand RNA 1 (FOXD2-AS1) was associated with the development of a number of tumors. However, whether FOXD2-AS1 is dysregulated in BC and its underlying mechanisms remain unclear. In the present study, it was identified that FOXD2-AS1 expression was upregulated in BC tissue, cell lines and sphere subpopulation. Additionally, the abnormal upregulation of FOXD2-AS1 predicted poor prognosis in patients with BC. Furthermore, downregulation of FOXD2-AS1 decreased cell proliferation, and migratory and invasive abilities in BC cells, and decreased the growth of transplanted tumors *in vivo*. Downregulation of FOXD2-AS1 decreased the percentage of CD44 antigen$^+$/signal transducer CD24$^-$ in breast cancer stem cell (BCSC) cells, and decreased the expression of numerous stem factors, including Nanog, octamer-binding transcription factor 4 (Oct4), and sex determining region Y-box 2 (SOX2), and inhibited the epithelial-mesenchymal transition process. FOXD2-AS1 was identified to be primarily located in the cytoplasm. Using bioinformatics analysis, a reporter gene assay and reverse transcription-polymerase chain reaction assays, it was demonstrated that microRNA (miR)-150-5p was able to bind directly with the 3'-untranslated region of FOXD2-AS1 and PFN2 mRNA. miR-150-5p mimics decreased the cell proliferation, migration and invasion of BC cells. FOXD2-AS1 knockdown significantly inhibited the miR-150-5p inhibitor-induced increase in Nanog, Oct4 and SOX2 expression. The miR-150-5p inhibitor-induced increase in N-cadherin, and decrease in E-cadherin and vimentin was inhibited by FOXD2-AS1 knockdown. Profilin 2 (PFN2) expression was significantly upregulated in BC tissues. Additionally, the abnormal upregulation of PFN2 was associated with poor prognosis in patients with BC. FOXD2-AS1 and PFN2 expression was positively correlated. Collectively, the present results demonstrated the role of the FOXD2-AS1/miR-150-5p/PFN2 axis in the development of BC, and provides novel targets for the treatment of BC, and potential biomarkers for diagnosis and prognosis of BC.

Correspondence to: Dr Xiang Ao or Dr Hongsheng Li, Department of Breast Surgery, Affiliated Cancer Hospital and Institute of Guangzhou Medical University, 78 Hengzhigang Road, Guangzhou, Guangdong 510095, P.R. China
E-mail: gyzlyyrxwk2018@163.com
E-mail: docli999@163.com

*Contributed equally

Key words: breast cancer, long non-coding RNA FOXD2 adjacent opposite strand RNA 1, microRNA150-5p, profilin 2, tumorigenesis

Introduction

Breast cancer (BC) is a common cancer and leading cause of cancer-associated mortality in women and is the second most lethal cancer worldwide, following lung adenocarcinoma (1,2). In the last decades, approaches used for the treatment of BC have advanced, including surgery, radiotherapy, chemotherapy and endocrine therapy, leading to a significant reduction of the rates of premature mortality (3). However, the molecular mechanisms responsible for BC development and progression remain unclear. There are diverse BC subtypes, and clear and definitive targets are limited, resulting in ambiguity of the pathophysiology of BC (4). It was demonstrated that, in response to therapy, distinct signaling pathways may be activated in different subtypes of BC (5,6). The features of tumorigenesis include uncontrolled cell proliferation, and high rates of metastasis and stemness (7,8). Therefore, determining the mechanisms of dysregulation of cell proliferation, metastasis and stemness is urgently required to identify key regulators in the development of BC and improve BC therapy.

Long non-coding RNAs (lncRNAs) are a family of transcripts, with lengths >200 nucleotides, which contain no open reading frames, and these RNAs are less abundant and more variable among tissues compared with mRNA expression (9). lncRNAs have been identified to serve key roles in the regulation of a broad array of cancer processes, including proliferation (10), apoptosis (11), metastasis (12) and drug resistance (13). lncRNAs may function through a wide range of mechanisms (14), including serving as signals, decoys, guides and scaffolds to modulate the transcriptional or post-transcriptional regulation of gene expression in multiple cancer types. Serving as guides or molecular scaffolds, lncRNAs

may recruit co-regulators of transcription to a specific DNA region or raise enzymes with chromatin-modifying activity to form ribonucleoprotein complexes, leading to the bridging of regulatory proteins and regulation of transcription (15). In addition, functioning as decoys, lncRNAs may bind directly with microRNAs (miRNAs) or proteins and thus modulate the functions of key regulators (16). Therefore, lncRNAs may serve an oncogenic or a tumor-suppressive role, making them good prognostic biomarkers and therapeutic targets.

lncRNA FOXD2 adjacent opposite strand RNA 1 (FOXD2-AS1; accession no. NR_026878), is located on chromosome 1p33 and consists of 2,527 nucleotides (17). It was firstly identified that FOXD2-AS1 expression is increased in gastric cancer (18,19). Previous studies demonstrated that FOXD2-AS1 is critical for cell proliferation, apoptotic cell death, invasion, migration and drug-resistance in non-small cell lung cancer (20), esophageal squamous cell carcinoma (21), nasopharyngeal carcinoma carcinogenesis (17), colorectal cancer (22) and bladder cancer (23). However, whether FOXD2-AS1 is dysregulated in BC and its underlying mechanisms remain unclear.

The present study aimed to identify the possible role of FOXD2-AS1 in the proliferation, migration, invasion and stemness in BC, and to clarify the clinical features of FOXD2-AS1 in BC. In the present study, an increased expression of FOXD2-AS1 was identified in BC tissues and cells. Critical roles of FOXD2-AS1 in the regulation of proliferation, epithelial-mesenchymal transition and stemness were identified. The results suggested that FOXD2-AS1 promoted BC malignancy and tumorigenesis by targeting the miRNA (miR)-150-5p/profilin 2 (PFN2) axis.

Materials and methods

Patients and tissue specimens. In total, 34 pairs of BC tissues and paired adjacent normal tissues were collected from the Department of Breast Surgery, Affiliated Cancer Hospital and Institute of Guangzhou Medical University (Guangzhou, China) between Jan 2012 and May 2012. The present study was approved by the Ethics Committee of the Affiliated Cancer Hospital and Institute of Guangzhou Medical University (approval no. ACHIGMU-2012-1-3-05). The specimens were immediately frozen in liquid nitrogen and subsequently stored at -80˚C for further determination. The female patients did not receive any radiation or chemotherapy prior to operation, and patients with hypertension and diabetes mellitus were excluded in the present study. All tissue sections were reviewed by at least two experienced pathologists. The tumor, node, metastasis (TNM) stage was evaluated according to the American Joint Committee on Cancer (24). Written informed consent was obtained from all the enrolled patients. A 5-year follow-up was performed and overall survival was defined as the length of time between surgery and mortality or the last follow-up (if mortality did not occur).

Cell lines, culture and transfection. A human normal breast epithelial cell line (MCF-10A) and human breast cancer cell lines (MCF-7, MDA-MB-231, MDA-MB-453 and MDA-MB-468) were purchased from The American Type Culture Collection (Manassas, VA, USA). The cell lines were incubated in RPMI-1640 medium (Corning, Inc., Corning, NY, USA) supplemented with 10% fetal bovine serum (FBS; Corning, Inc.) and cultured at 37˚C with 5% CO_2. Cells in the exponential phase were used in the experiments. Small interfering RNA (siRNA) targeting FOXD2-AS1 (cat. no. 4390771; 100 nM) and its scrambled control siRNA (cat. no. AM4636; 100 nM) (Thermo Fisher Scientific, Inc., Waltham, MA, USA) were employed to downregulate FOXD2-AS1. Short hairpin RNA (shRNA) targeting FOXD2-AS1 (100 nM) was prepared based on those siRNAs using pSilencer 3.1-H1 puro plasmids (Shanghai GenePharma Co. Ltd., Shanghai, China). Lentivirus carrying shRNA targeting FOXD2-AS1 ($1x10^7$ IFU/ml) was constructed using pre-packaged lentivirus (Shanghai GenePharma Co. Ltd.). The miR-150-5p mimics (cat. no. 4464084; 100 nM), inhibitors (cat. no. 4464066; 100 nM) and scrambled control oligonucleotides (cat. nos. 4464059 and 4464076; 100 nM) were purchased from Thermo Fisher Scientific, Inc. Oligonucleotide and lentivirus transfection into cells were conducted using Lipofectamine® 2000 (Invitrogen; Thermo Fisher Scientific, Inc.) according to the manufacturer's protocol. After 48 h of transfection, subsequent experiments were performed.

Cell proliferation. Cell proliferation was determined by Cell Counting Kit-8 (CCK-8; Beyotime Institute of Biotechnology, Haimen, China), according to the manufacturer's protocol. Following the treatment, cells were incubated in 10 μl CCK-8 solution for 1 h at 37˚C. Finally, the absorbance at 450 nm was measured following the plate incubation at 37˚C for 2 h (Bio-Rad Laboratories, Inc., Hercules, CA, USA). Triplicate experiments were performed.

RNA extraction and reverse transcription-quantitative polymerase chain reaction (RT-qPCR). Tissues and cells were lysed and total RNA was extracted using TRIzol® (Thermo Fisher Scientific, Inc.) reagent, according to the manufacturer's protocol. RNA quality was measured using Nanodrop equipment (Thermo Fisher Scientific, Inc., Wilmington, DE, USA). For the detection of mRNA and lncRNA, 500 ng RNA was reverse transcribed into cDNA using a cDNA synthesis kit (Thermo Fisher Scientific, Inc.) according to the following conditions: 65˚C for 5 min, 25˚C for 10 min, 50˚C for 15 min and 85˚C for 5 min. The sequences of specific primers used for RT-qPCR were as follows: GAPDH, forward, 5'-GCGAGATC GCACTCATCATCT-3' and reverse, 5'-TCAGTGGTGGACCT GACC-3'; FOXD2-AS1, forward, 5'-TGGACCTAGCTGCAGC TCCA-3' and reverse, 5'-AGTTGAAGGTGCACACACTG-3'; E-cadherin, forward, 5'-CTGCTGCAGGTCTCCTCTTG-3' and reverse, 5'-TGTCGACCGGTGCAATCTTC-3; Vimentin, forward, 5'-AAGGCGAGGAGAGCAGGATT-3' and reverse, 5'-GGTCATCGTGATGCTGAGAAG-3'; N-cadherin, forward, 5'-GTGCCATTAGCCAAGGGAATTCAGC-3' and reverse, 5'-GCGTTCCTGTTCCACTCATAGGAG-3'; Nanog, forward, 5'-GGTCCCAGTCAAGAAACAGA-3' and reverse, 5'-GAG GTTCAGGATGTTGGAGA-3'; Oct4, forward, 5'-CCCGAAA GAGAAAGCGAACC-3' and reverse, 5'-GCAGCCTCAAAA TCCTCTCG-3'; and Sox2, forward, 5'-CATGTCCCAGCACTA CCAGA-3' and reverse, 5'-TTTGAGCGTACCGGGTTTTC-3'. Reactions of RT-qPCR were conducted on an ABI 7500 real-time PCR System (Applied Biosystems; Thermo Fisher

Scientific, Inc.). GAPDH was used as an internal control for normalization.

For the detection of miRNA, the qScript miRNA cDNA Synthesis kit (Quantabio, Beverly, MA, USA) was employed to synthesize cDNA, according to the following conditions: 50˚C for 60 min and 85˚C for 5 sec. miRNA RT-qPCR was performed using a miScript SYBR Green PCR kit (Qiagen GmbH, Hilden, Germany) according to the manufacturer's protocol. The sequences of specific primers used for RT-qPCR were as follows: U6, forward, 5'-CTCGCTTCGGCAGCACA-3'; reverse, 5'-AACGCTTCACGAATTTGCGT-3'; miR-150-5p, forward, 5'-TCTCCCAACCCTTGTACCAGTG-3'; reverse, 5'-CTCAACTGGTGTCGTGGTA-3'. U6 was used as an internal control for normalization. The level of target gene was calculated relative to internal control using the $2^{-\Delta\Delta Cq}$ method (25). The PCR conditions were as follows: 95˚C for 5 min, 40 cycles of 95˚C for 20 sec and 62˚C for 30 sec, followed by 72˚C for 3 min.

Cytoplasmic and nuclear isolation of RNA. The location of lncRNA FOXD2-AS1 was measured using the Cytoplasmic and Nuclear RNA Purification kit (Norgen Biotek Corp., Thorold, ON, Canada) according to the manufacturer's protocol.

Luciferase reporter assay. The fragments of wild-type (WT) or mutated (MUT) 3'untranslated region (UTR) of FOXD2-AS1 and PFN2 were synthesized, inserted into the vector pGL3 (Shanghai GeneChem Co. Ltd., Shanghai, China), and subsequently miR-150-5p mimics and their respective control were transfected into 293T cells (American Type Culture Collection) using Lipofectamine® 2000 (Invitrogen; Thermo Fisher Scientific, Inc.). The *Renilla* luciferase plasmid was used for normalization. The luciferase activity was measured using the Dual-Luciferase Reporter Assay System (Promega Corporation, Madison, WI, USA) according to the manufacturer's protocol. After 48 h of transfection relative luciferase activity was calculated by comparison with *Renilla* luciferase activity.

Sphere-formation assay. The formation of spheres was evaluated as previously described (26). BC cells were suspended and $5x10^4$ cells/well were seeded into 6-well plates (Corning, Inc.). In total, 2 ml serum-free Dulbecco's modified Eagle's medium (DMEM; Gibco; Thermo Fisher Scientific, Inc.) was added to each well to re-suspend cells. The medium contained 4 U/l insulin, 20 mg/l epidermal growth factor and 20 mg/l human fibroblast growth factor. Sphere-formation was observed using a light microscope (magnification, x400) and the number of spheroids was counted (Olympus Corporation, Tokyo, Japan).

Flow cytometry analysis. CD44 antigen $(CD44)^+$/signal transducer $CD24\ (CD24)^-$ cells percentage was determined using a Breast Cancer Stem Cell Isolation kit (R&D Systems Inc., Minneapolis, MN, USA) using flow cytometer analysis. Cells were trypsinized and resuspended to a density of $2x10^5$ cells/well. Cells were incubated in PBS containing 2% FBS and human CD24 biotinylated antibody, human CD44 biotinylated antibody, human CD24 detection antibody and human CD44 detection antibody provided in the kit for 15 min at 2-8˚C. A flow cytometer was used (BD Biosciences, Franklin Lakes, NJ, USA) and $CD44^+/CD24^-$ cells percentage was measured (Kaluza 1.2 software; Beckman Coulter, Inc., Brea, CA, USA).

Bioinformatics analysis. The lncRNA-miRNA interaction prediction was performed using StarBase v 2.0 (http://starbase.sysu.edu.cn/starbase2). The miRNA-mRNA interaction prediction was conducted using TargetScanHuman 7.1 (http://www.targetscan.org/vert_71/).

Migration and invasion assays. A wound healing assay was conducted to evaluate the migration of the cells. $5x10^5$ cells were plated in 6-well plates and when cells were grown to 90% confluence, a scratch was made through the monolayer using a sterile pipette tip. The floating cells were removed with PBS and subsequently, cells were cultured in serum-free medium. Images were captured at 0 and 24 h. The width of the scratches at 0 and 24 h was measured. The migration distance was calculated following the formula: Migration rate = migration distance/original distance. Relative migration distance was expressed as fold-change of the control.

A Matrigel assay was conducted to evaluate the invasion of the cells. $1x10^5$ cells in 200 μl serum-free medium were added to the upper chamber of Transwell chambers (Corning, Inc.) were coated with DMEM-diluted Matrigel (BD Biosciences). In total, 800 μl medium containing 10% FBS was added to the lower chamber. Following incubation at 37˚C for 48 h, the upper membrane surface was scraped using a cotton tip to remove non-invaded cells. Finally, the membrane was fixed with 4% paraformaldehyde for 30 min at room temperature and stained with 1% crystal violet for 15 min at room temperature. Staining was observed using a light microscope (magnification, x400; Olympus Corporation) and the number of invaded cells was counted and expressed as the fold-change of the control.

Nude mice experiments. Xenograft mice were established as per the experimental protocols and the study was approved by the Affiliated Cancer Hospital and Institute of Guangzhou Medical University. The mice were housed in a specific pathogen-free animal laboratory under temperature (23±2˚C) and humidity (55±5%) condition with a standard light cycle (12 h light/dark) and free access to food and water. In total, 12 female BALB/c nu/nu mice (4-weeks; weighing 16±2 g; purchased from The Animal Centre of Guangzhou Medical University) were randomly divided into two groups with six mice in each group. In total, $1x10^7$ MCF-7 cells were suspended in physiological saline. An equal volume of Matrigel (Corning, Inc.) was added to the cell suspension. Each mouse was subcutaneously injected with 150 μl mixture to generate a tumor. 17b-Estradiol pellets (0.72 mg; 60 day release; Innovative Research of America, Sarasota, FL, USA) were implanted subcutaneously using a precision trochar (10 gages) at the time of cell injection. The tumor size was measured using a caliper every 3 days and the volume of the tumor was calculated using the following formula: Volume = (length/2) x $width^2$. The experimental period was 21 days. Subsequently, the mice were sacrificed, and tumors

Table I. Association between FOXD2-AS1 expression and clinicopathological characteristics of patients with breast cancer.

Clinicopathological characteristics	Number of patients	FOXD2-AS1 expression		P-value
		Low, n=15	High, n=19	
Age				
<50	18	8	9	0.327
≥50	16	7	10	
ER				
Positive	23	8	14	0.006[a]
Negative	11	7	5	
PR				
Positive	19	9	9	0.623
Negative	15	6	10	
HER2				
Positive	20	9	13	0.025[a]
Negative	14	6	6	
EGFR				
Positive	18	8	9	0.712
Negative	16	7	10	
Distant metastases				
Yes	21	7	14	0.017[a]
No	13	8	5	
Lymphatic metastasis				
Positive	22	8	15	0.008[a]
Negative	12	7	4	
TNM stage				
I-II	20	9	12	0.013[a]
III	14	6	7	

[a]P<0.05. TNM, tumor, node, metastasis; FOXD2-AS1, FOXD2 adjacent opposite strand RNA 1; ER, estrogen receptor; PR, progesterone receptor; HER2, human epidermal growth factor receptor 2; EGFR, epidermal growth factor receptor.

were resected and weighed. Tumor tissues were stored at -80˚C for further analysis.

Statistical analysis. The data are presented as the mean ± standard deviation. A total of three independent experiments were performed. Differences between two groups were analyzed with Student's t-test. Differences among more than two groups were analyzed with analysis of variance followed by Tukey's test. Overall survival was analyzed using the Kaplan-Meier method and log-rank test. P<0.05 was considered to indicate a statistically significant difference. GraphPad Prism 6.01 software (GraphPad Software, Inc., La Jolla, CA, USA) was used to perform statistical analyses.

Results

lncRNA FOXD2-AS1 expression is increased in BC tissues and is associated with poor prognosis. To examine the pattern of lncRNA FOXD2-AS1 expression in BC tissues and non-tumor tissues, the mRNA expression of FOXD2-AS1 in 34 paired BC tissues and adjacent normal tissues was determined. The results demonstrated that mRNA expression of FOXD2-AS1 was significantly increased in BC tissue samples, compared with adjacent normal tissues (Fig. 1A and B; P<0.01). According to the median expression (6.9) of FOXD2-AS1, the BC tissues specimens were divided into two groups: A higher FOXD2-AS1 expression group and the other group with lower expression of FOXD2-AS1 (Fig. 1C). The differences of overall survival between groups with either higher or lower expression of FOXD2-AS1 were compared, using Kaplan-Meier curves and a log-rank test. The results demonstrated that the overall survival was poor in patients with BC with high expression levels of FOXD2-AS1, compared with patients with low expression levels of FOXD2-AS1 (Fig. 1D). The clinicopathologic features of the patients are presented in Table I. It was demonstrated that higher FOXD2-AS1 expression was associated the positive expression of estrogen receptor, human epidermal growth factor receptor 2, distant metastases, lymphatic metastasis and tumor, node, metastasis stage. Overall, the present results suggested that FOXD2-AS1 expression was increased in BC tissues and upregulation of FOXD2-AS1 was associated with a poor prognosis BC. The

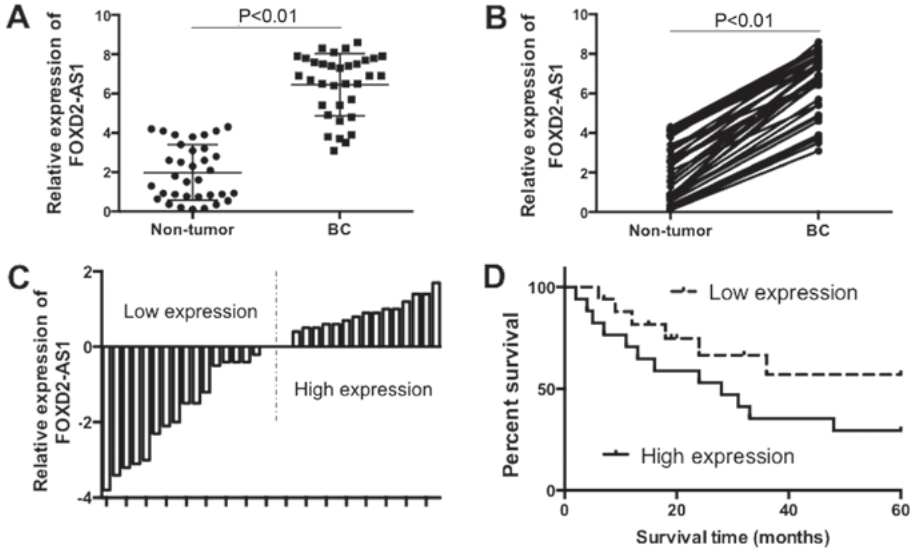

Figure 1. FOXD2-AS1 expression is increased in BC tissues and was associated with poor prognosis of BC. (A) Expression of FOXD2-AS1 in 34 pairs of BC tissues and paired adjacent non-tumor tissue was determined by reverse transcription-quantitative polymerase chain reaction. (B) Respective association of FOXD2-AS1 expression between each BC tissue specimen and paired adjacent normal tissue. (C) In total, 34 tissues samples were divided into two groups: Higher FOXD2-AS1 expression group and lower FOXD2-AS1 expression group, according to the median expression of FOXD2-AS1. (D) Overall survival in patients with BC with high/low FOXD2-AS1 expression levels. BC, breast cancer; FOXD2-AS1, FOXD2 adjacent opposite strand RNA 1.

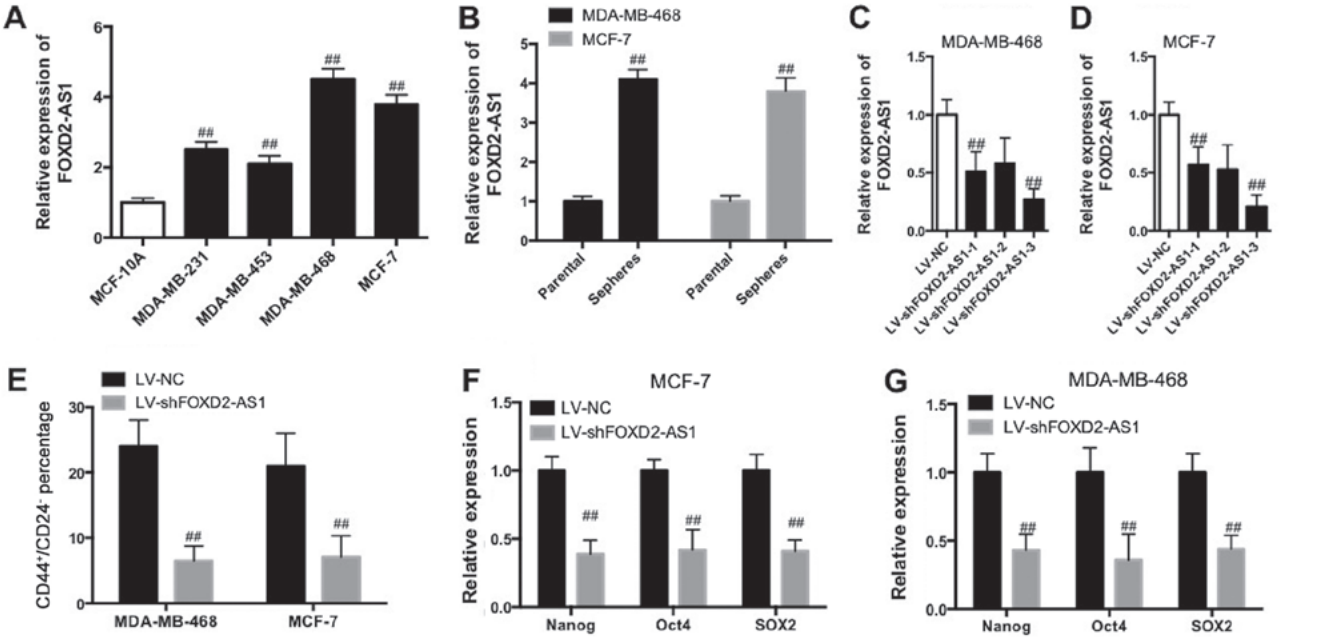

Figure 2. FOXD2-AS1 knockdown reduces BCSC properties in BC cells. (A) RT-qPCR determination of FOXD2-AS1 in BC cell lines, MCF-7, MDA-MB-231, MDA-MB-453 and MDA-MB-468, and human normal breast epithelial cells (MCF-10A). ##P<0.01 vs. MCF-10A. (B) Expression of FOXD2-AS1 in MCF-7 and MDA-MB-468 spheres and parental cells was determined using RT-qPCR. ##P<0.01 vs. respective parental. Knockdown efficiency of FOXD2-AS1 in (C) MDA-MB-468 and (D) MCF-7 cells. (E) Percentage of $CD44^+/CD24^-$ cells in BCSC cells (MCF-7 and MDA-MB-468) was analyzed by flow cytometry. Expression of stem factors (Nanog, Oct4, SOX2) in (F) MCF-7 and (G) MDA-MB-468 cells with downregulation of FOXD2-AS1 was determined using RT-qPCR. ##P<0.05 vs. respective LV-NC. FOXD2-AS1, FOXD2 adjacent opposite strand RNA 1; BCSC, breast cancer stem cell; BC, breast cancer; RT-qPCR, reverse transcription-quantitative polymerase chain reaction; CD44, CD44 antigen; CD24, signal transducer CD24; Oct4, octamer-binding transcription factor 4; SOX2, sex determining region Y-box 2; LV, lentivirus; NC, negative control; sh, small hairpin.

results demonstrated that FOXD2-AS1 may serve an oncogenic role in the tumorigenesis of BC.

FOXD2-AS1 knockdown reduces the breast cancer stem cell (BCSC) properties. It was investigated whether FOXD2-AS1 served a role in the maintenance of BCSC properties in BC. The FOXD2-AS1 expression level was significantly increased in BC cell lines, MCF-7, MDA-MB-231, MDA-MB-453 and MDA-MB-468, compared with normal human breast epithelial cells (MCF-10A; Fig. 2A; P<0.01). Furthermore, the FOXD2-AS1 expression level was significantly increased in MCF-7 and MDA-MB-468 sphere cells compared with

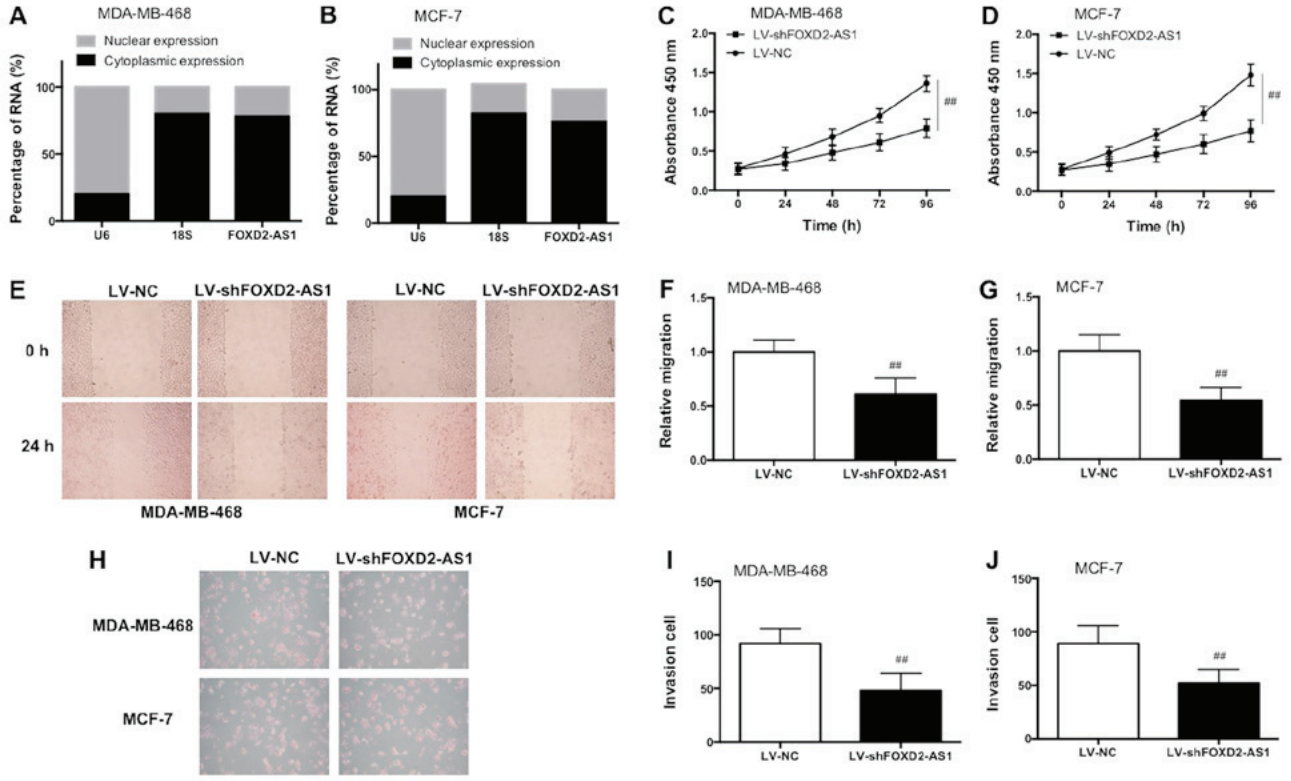

Figure 3. FOXD2-AS1 downregulation inhibits the proliferation, invasion and migration in breast cancer stem cells. Subcellular localization of FOXD2-AS1 in (A) MDA-MB-468 and (B) MCF-7 cells was detected. Effect of FOXD2-AS1 downregulation on proliferation in (C) MDA-MB-468 and (D) MCF-7 cells was examined by a Cell Counting Kit-8 assay. (E) Representative images of the wound-healing assay. Magnification, x400. Effect of FOXD2-AS1 downregulation on migration in (F) MDA-MB-468 and (G) MCF-7 cells was determined by a wound-healing assay. (H) Representative images of the Matrigel assay. Effect of FOXD2-AS1 downregulation on invasion in (I) MDA-MB-468 and (J) MCF-7 cells was determined by a Matrigel assay. Data are presented as the mean ± standard deviation. $^{\#\#}$P<0.05 vs. LV-NC. FOXD2-AS1, FOXD2 adjacent opposite strand RNA 1; LV, lentivirus; NC, negative control; sh, small hairpin.

parental cells (Fig. 2B; P<0.01). BCSC cells [MCF-7 cancer stem cells (CSCs) and MDA-MB-468 CSCs] were transfected with lentivirus-mediated interfering oligonucleotides targeting FOXD2-AS1 to knockdown the expression of FOXD2-AS1 (Fig. 2C and D). Knockdown of FOXD2-AS1 significantly decreased the percentage of $CD44^+/CD24^-$ in the BCSC cell (MCF-7 CSC and MDA-MB-468 CSC) subpopulation (Fig. 2E; P<0.01). The results additionally demonstrated that downregulation of FOXD2-AS1 resulted in a significant decrease of stem factor expression, including Nanog, octamer-binding transcription factor 4 (Oct4) and sex determining region Y-box 2 (SOX2; Fig. 2F and G; P<0.01). Therefore, the data suggested that knockdown of FOXD2-AS1 decreased the properties of BCSC.

Knockdown of FOXD2-AS1 inhibits the proliferation, migration and invasion of BC cells in vitro. The nuclear and cytoplasmic expression of FOXD2-AS1 was measured and it was identified that FOXD2-AS1 was primarily located in the cytoplasm in MCF-7 and MDA-MB-468 cells (Fig. 3A and B). Knockdown of FOXD2-AS1 inhibited cell proliferation in MCF-7 and MDA-MB-468 cells, as demonstrated by the CCK-8 results (Fig. 3C and D). As demonstrated in the wound-healing assay, FOXD2-AS1 knockdown significantly decreased the relative distance of migration (Fig. 3E-G; P<0.01). As demonstrated in the Matrigel assay, knockdown of FOXD2-AS1 decreased the number of invaded cells (Fig. 3H-J). Taken together, the data demonstrated that knockdown of FOXD2-AS1 suppressed the proliferation, invasion and migration of BC cells *in vitro*.

Knockdown of FOXD2-AS1 suppresses BC tumor growth in vivo. To investigate the role of FOXD2-AS1 downregulation on BC growth, a xenograft mice *in vivo* assay was conducted. The knockdown of FOXD2-AS1 significantly decreased the tumor volume in xenograft mice (Fig. 4A; P<0.01). Additionally, knockdown of FOXD2-AS1 significantly decreased the weight of the tumor (Fig. 4B; P<0.01). The expression levels of Nanog, Oct4 and SOX2 were significantly decreased by FOXD2-AS1 downregulation (Fig. 4C; P<0.01). Furthermore, it was demonstrated that FOXD2-AS1 knockdown significantly decreased N-cadherin expression, and increased E-cadherin and vimentin expression (Fig. 4D; P<0.01). Therefore, the data suggested that FOXD2-AS1 knockdown suppressed the tumor growth of BC *in vivo*.

FOXD2-AS1 promotes BC through modulation of PFN2 by sponging miR-150-5p. To examine the molecular mechanism underlying FOXD2-AS1-exhibited regulation of proliferation, invasion, migration and BCSC properties of BC, the possible targets of FOXD2-AS1 were investigated. Using bioinformatics analysis and validation assays, it was identified that there were complementary binding sites between miR-150-5p and the 3'-UTR of FOXD2-AS1 (Fig. 5A). The results of the reporter gene assay provided evidence that miR-150-5p was able to bind with the FOXD2-AS1 3'-UTR (Fig. 5B).

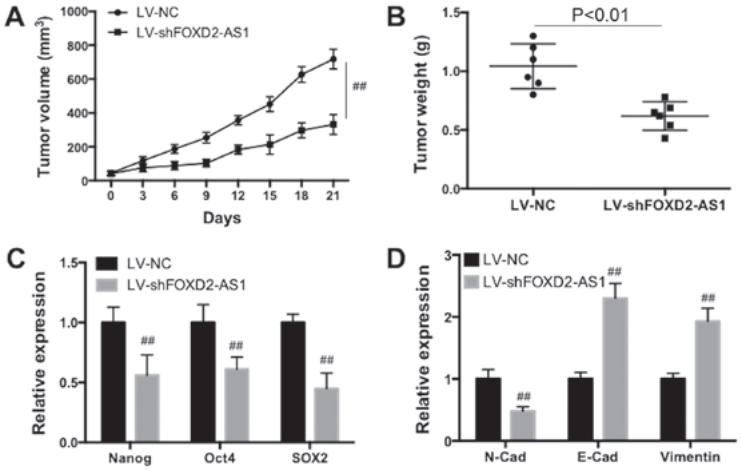

Figure 4. FOXD2-AS1 downregulation suppresses the tumor growth of breast cancer *in vivo*. (A) Tumor volume was measured in transplanted mice. (B) Tumor weight was determined. (C) Expression of Nanog, Oct4 and SOX2 was determined using RT-qPCR. (D) Expression of N-Cad, E-Cad and vimentin was determined using RT-qPCR. Data are presented as the mean ± standard deviation. $^{\#\#}$P<0.05 vs. respective LV-NC. FOXD2-AS1, FOXD2 adjacent opposite strand RNA 1; RT-qPCR, reverse transcription-quantitative polymerase chain reaction; Oct4, octamer-binding transcription factor 4; SOX2, sex determining region Y-box 2; Cad, cadherin; LV, lentivirus; NC, negative control; sh, small hairpin.

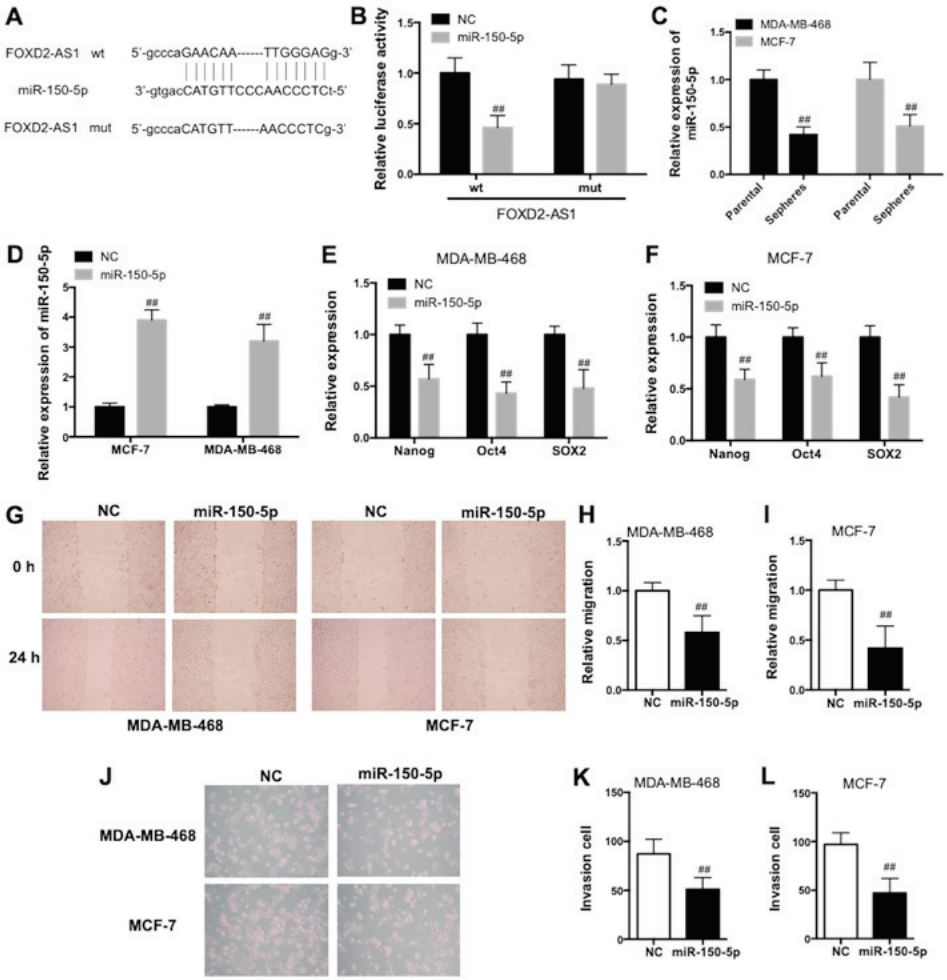

Figure 5. FOXD2-AS1 regulates BC malignancy through interaction with miR-150-5p. (A) Bioinformatics analysis of the binding between miR-150-5p and 3'UTR of wt FOXD2-AS1 and the mutation of putative binding sites. (B) Direct binding of miR-150-5p with FOXD2-AS1 3'-UTR was detected by a luciferase reporter assay. (C) RT-qPCR determination of miR-150-5p in MDA-MB-468 and MCF-7 spheres and parental cells. $^{\#\#}$P<0.01 vs. respective parental. (D) MDA-MB-468 and MCF-7 cells were transfected with miR-150-5p mimics and transfection efficiency was evaluated. MDA-MB-468 and MCF-7 cells were transfected with miR-150-5p mimics. RT-qPCR determination of Nanog, Oct4 and SOX2 in (E) MDA-MB-468 and (F) MCF-7 cells. (G) Representative images of the wound-healing assay. Magnification, x400. Migration in (H) MDA-MB-468 and (I) MCF-7 cells was determined by a wound-healing assay. (J) Representative images of the Matrigel assay. Invasion of (K) MDA-MB-468 and (L) MCF-7 cells was determined by a Matrigel assay. $^{\#\#}$P<0.05 vs. respective NC. FOXD2-AS1, FOXD2 adjacent opposite strand RNA 1; BC, breast cancer; miR, microRNA; UTR, untranslated region; wt, wild-type; RT-qPCR, reverse transcription-quantitative polymerase chain reaction; Oct4, octamer-binding transcription factor 4; SOX2, sex determining region Y-box 2; NC, negative control; mut, mutant.

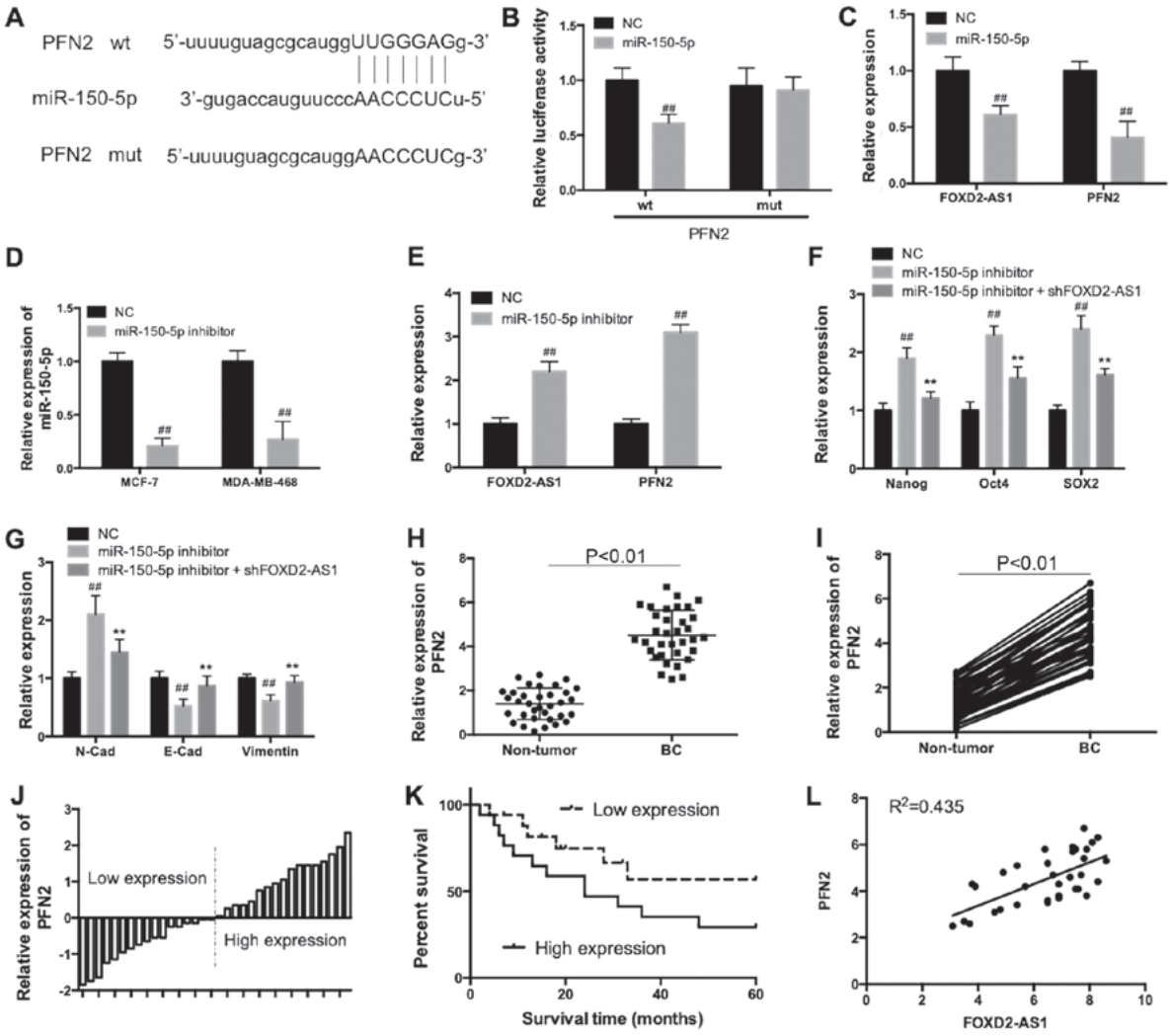

Figure 6. FOXD2-AS1 modulated the expression of PFN2 by sponging miR-150-5p. (A) Bioinformatics analysis of the binding between miR-150-5p and 3'UTR of wt PFN2 and the mutation of putative binding sites. (B) Direct binding of miR-150-5p with PFN2 3'-UTR was detected by a luciferase reporter assay. (C) RT-qPCR determination of FOXD2-AS1 and PFN2 expression in MCF-7 cells following transfection of miR-150-5p mimics. (D) MCF-7 cells were transfected with miR-150-5p inhibitors and the transfection efficiency was examined. (E) RT-qPCR determination of FOXD2-AS1 and PFN2 expression in MCF-7 cells following transfection of miR-150-5p inhibitors. MCF-7 cells were transfected with miR-150-5p inhibitors in the presence or absence of lentivirus-shFOXD2-AS1. (F) RT-qPCR determination of Nanog, Oct4 and SOX2. (G) RT-qPCR determination of N-Cad, E-Cad and vimentin. (H) RT-qPCR determination of PFN2 in 34 pairs of BC tissues and paired adjacent normal tissues. (I) Respective association of PFN2 expression between each BC tissue specimen and paired adjacent normal tissue. (J) A total of 34 tissues samples were divided into two groups: Higher PFN2 expression group and lower PFN2 expression group, according to the median expression of PFN2. (K) Overall survival in patients with BC with high/low PFN2 expression levels. (L) Correlation between FOXD2-AS1 and PFN2 expression in BC tissues. $^{\#\#}$P<0.05 vs. respective NC; **P<0.05 vs. respective miR-150-5p inhibitor. FOXD2-AS1, FOXD2 adjacent opposite strand RNA 1; PFN2, profilin 2; miR, microRNA; UTR, untranslated region; wt, wild-type; RT-qPCR, reverse transcription-quantitative polymerase chain reaction; sh, small hairpin; Oct4, octamer-binding transcription factor 4; SOX2, sex determining region Y-box 2; BC, breast cancer; NC, negative control; mut, mutant; Cad, cadherin.

The expression of miR-150-5p was lower in MDA-MB-468 and MCF-7 sphere cells compared with respective parental cells (Fig. 5C). Transfection of miR-150-5p mimics (Fig. 5D) significantly decreased mRNA expression levels of Nanog, Oct4 and SOX2 in MDA-MB-468 and MCF-7 cells (Fig. 5E and F; P<0.01). As observed in the wound-healing assay, miR-150-5p mimics significantly decreased the relative migration distance, demonstrating a decrease in migratory ability (Fig. 5G-I; P<0.01). As demonstrated in the Matrigel assay, miR-150-5p mimics decreased the number of invaded cells, suggesting a reduction of invasive ability (Fig. 5J-L). Taken together, these data demonstrated that miR-150-5p inhibited the proliferation, invasion, migration and BCSC properties of BC *in vitro*.

Using bioinformatics analysis, it was identified that there were complementary binding sites between miR-150-5p and the PFN2 3'-UTR (Fig. 6A). Furthermore, the direct interaction between miR-150-5p and PFN2 3'-UTR was confirmed by the results of the luciferase reporter assay (Fig. 6B). Transfection of miR-150-5p mimics decreased FOXD2-AS1 and PFN2 expression (Fig. 6C), whereas, miR-150-5p inhibitors (Fig. 6D) increased FOXD2-AS1 and PFN2 expression (Fig. 6E). FOXD2-AS1 knockdown significantly inhibited miR-150-5p inhibitor-induced increase of Nanog, Oct4 and SOX2 expression (Fig. 6F; P<0.01). Additionally, the miR-150-5p inhibitor-induced increase of N-cadherin, and decrease of E-cadherin and vimentin was inhibited by FOXD2-AS1 knockdown (Fig. 6G).

Figure 7. Schematic figure of FOXD2-AS1-miR-150-5p/PFN2-induced promotion of BC. FOXD2-AS1 promotes BC proliferation, invasion, migration, stemness and tumor growth. FOXD2-AS1 regulates BC malignancy through modulation of PFN2 by sponging miR-150-5p. The FOXD2-AS1/miR-150-5p/PFN2 axis is critical in the development of BC. FOXD2-AS1, FOXD2 adjacent opposite strand RNA 1; miR, microRNA; PFN2, profilin 2; BC, breast cancer.

The expression of PFN2 was significantly increased in BC tissues specimens compared with adjacent normal tissues (Fig. 6H and I; P<0.01). According to the median expression of PFN2 (4.35), the BC tissues specimens were divided into two groups: A higher PFN2 expression group and the other group with lower expression of PFN2 (Fig. 6J). The differences of overall survival between groups with either higher or lower expression of PFN2 were compared using Kaplan-Meier curves and a log-rank test. The results demonstrated that overall survivals were poor in patients with BC with high expression levels of PFN2, compared with patients with low expression levels of PFN2 (Fig. 6K). Furthermore, the expression of FOXD2-AS1 was positively correlated with the PFN2 expression level in tumor tissues of patients with BC (Fig. 6L). The present results concluded that FOXD2-AS1 promoted BC through modulation of PFN2 by sponging miR-150-5p (Fig. 7).

Discussion

BC is one of the most prevalent malignant tumors in women worldwide and one of the leading causes of cancer mortality (27). The high rate of metastasis and recurrence of BC typically contribute to accelerated progression (28). lncRNAs are emerging as important regulators in the process of cancer stemness and tumorigenesis (12,29). In the present study, it was demonstrated that FOXD2-AS1 expression was significantly increased in BC tissue, cells and sphere subpopulation. Additionally, the upregulation of FOXD2-AS1was closely associated with poor prognosis of patients with BC. Furthermore, downregulation of FOXD2-AS1 decreased cell proliferation, migration and invasion in BC cells, and inhibited tumor growth in the transplanted tumor *in vivo*. Knockdown of FOXD2-AS1 decreased the percentage of $CD44^+/CD24^-$ cells and the ability to form spheres in the BCSC cell (MCF-7 CSC and MDA-MB-468 CSC) subpopulation, suggesting the inhibitory role of FOXD2-AS1 knockdown in BC stemness. Furthermore, knockdown of FOXD2-AS1 decreased the expression of stem factors, including Nanog, Oct4 and SOX2. It was identified that CSCs limit the efficiency of surgical resection or post-chemoradiotherapy as these cells may endow the growth or proliferation potential (30,31). The results suggested that FOXD2-AS1 serves an oncogenic role in BC and high FOXD2-AS1 expression was associated with poor prognosis of patients with BC.

FOXD2-AS1 was primarily located in the cytoplasm, suggesting that the primary reason for FOXD2-AS1-exhibited regulation of BC malignancy was due to post-transcriptional regulation. At present, serving as an miRNA 'sponge' is believed to be the most prevalent mechanism of lncRNA-mediated biological regulation (32). In the present study, it was demonstrated that the expression of FOXD2-AS1 was increased in the sphere subpopulation of BCSC, and FOXD2-AS1 and PFN2 expression was positively correlated. Furthermore, it was identified that miR-150-5p targeted the 3'-UTR of FOXD2-AS1 and PFN2 mRNA, and miR-150-5p expression was negatively associated with FOXD2-AS1 and PFN2 expression. miR-150-5p mimics decreased cell proliferation, migration and invasion in BC cells. Additionally, PFN2 expression was significantly upregulated in BC tissues. Furthermore, the upregulation of PFN2 indicated poor prognosis of patients with BC. FOXD2-AS1 and PFN2 expression was positively correlated. Previous studies demonstrated that miR-150-5p and PFN2 were able to regulate the development of certain cancer types (33-35). miR-150-5p inhibits cancer cell aggressiveness by targeting SPARC (osteonectin), cwcv and kazal like domain proteoglycan 1 in head and neck squamous cell carcinoma (33). PFN2 was correlated with poor prognosis of esophageal squamous cell carcinoma, which is proposed to be a therapeutic target (34). It was additionally demonstrated that PFN2 promoted migration, invasion and stemness of HT29 human colorectal cancer stem cells (35). However, at present, to the best of the authors' knowledge, there is no evidence for the direct interaction between FOXD2-AS1, miR-150-5p and PFN2. In summary, all the data suggested that FOXD2-AS1 regulated the expression of PFN2 and BCSC by serving as a sponge of miR-150-5p.

In conclusion, the findings demonstrated that FOXD2-AS1 was crucial for BC proliferation, invasion, migration and stemness, and tumor growth. FOXD2-AS1 regulates BC malignancy through modulation of PFN2 by sponging miR-150-5p. The present results suggested that the FOXD2-AS1/miR-150-5p/PFN2 axis is involved in the development of BC, and provides novel targets for the treatment of BC, and potential biomarkers for the diagnosis and prognosis of BC.

Acknowledgements

Not applicable.

Funding

The present study was supported by General Project of Western Medicine of Guangzhou Health and Family Planning Commission (grant no. 20181A011099), Natural Science Foundation of Guangdong Province (grant no. 22017A030313551) and Guangzhou Key Medical Discipline Construction Project Fund.

Availability of data and materials

The datasets generated and/or analyzed during the current study are available from the corresponding author on reasonable request.

Authors' contributions

XA, MJ and NQ designed the study and wrote the paper. MJ, NQ, HX, HLia and HLi performed the experiments and analyzed the data. All authors read and approved the final manuscript.

Ethics approval and consent to participate

The present patient and animal studies were approved by the Ethics Committee of the Affiliated Cancer Hospital and Institute of Guangzhou Medical University (approval no. ACHIGMU-2012-1-3-05; Guangzhou, China). Written informed consent was obtained from all the enrolled patients.

Patient consent for publication

Not applicable.

Competing interests

The authors declare that they have no competing interests.

References

1. Ferlay J, Soerjomataram I, Dikshit R, Eser S, Mathers C, Rebelo M, Parkin DM, Forman D and Bray F: Cancer incidence and mortality worldwide: Sources, methods and major patterns in GLOBOCAN 2012. Int J Cancer 136: E359-E386, 2015.
2. Landero J, Touloei K and Glick BP: Invasive ductal breast carcinoma underneath a lipoma in a male patient. J Clin Aesthet Dermatol 5: 33-37, 2012.
3. Hurvitz SA, Hu Y, O'Brien N and Finn RS: Current approaches and future directions in the treatment of HER2-positive breast cancer. Cancer Treat Rev 39: 219-229, 2013.
4. Jia T, Zhang L, Duan Y, Zhang M, Wang G, Zhang J and Zhao Z: The differential susceptibilities of MCF-7 and MDA-MB-231 cells to the cytotoxic effects of curcumin are associated with the PI3K/Akt-SKP2-Cip/Kips pathway. Cancer Cell Int 14: 126, 2014.
5. Jovanovic J, Rønneberg JA, Tost J and Kristensen V: The epigenetics of breast cancer. Mol Oncol 4: 242-254, 2010.
6. Parton M, Dowsett M and Smith I: Studies of apoptosis in breast cancer. BMJ 322: 1528-1532, 2001.
7. Hanahan D and Weinberg RA: The hallmarks of cancer. Cell 100: 57-70, 2000.
8. Kim K, Chie EK, Han W, Noh DY, Oh DY, Im SA, Kim TY, Bang YJ and Ha SW: Prognostic factors affecting the outcome of salvage radiotherapy for isolated locoregional recurrence after mastectomy. Am J Clin Oncol 33: 23-27, 2010.
9. Mercer TR, Dinger ME and Mattick JS: Long non-coding RNAs: Insights into functions. Nat Rev Genet 10: 155-159, 2009.
10. Prensner JR, Iyer MK, Sahu A, Asangani IA, Cao Q, Patel L, Vergara IA, Davicioni E, Erho N, Ghadessi M, *et al*: The long noncoding RNA SChLAP1 promotes aggressive prostate cancer and antagonizes the SWI/SNF complex. Nat Genet 45: 1392-1398, 2013.
11. Huarte M, Guttman M, Feldser D, Garber M, Koziol MJ, Kenzelmann-Broz D, Khalil AM, Zuk O, Amit I, Rabani M, *et al*: A large intergenic noncoding RNA induced by p53 mediates global gene repression in the p53 response. Cell 142: 409-419, 2010.
12. Gupta RA, Shah N, Wang KC, Kim J, Horlings HM, Wong DJ, Tsai MC, Hung T, Argani P, Rinn JL, *et al*: Long non-coding RNA HOTAIR reprograms chromatin state to promote cancer metastasis. Nature 464: 1071-1076, 2010.
13. Fan Y, Shen B, Tan M, Mu X, Qin Y, Zhang F and Liu Y: Long non-coding RNA UCA1 increases chemoresistance of bladder cancer cells by regulating Wnt signaling. FEBS J 281: 1750-1758, 2014.
14. Wang KC and Chang HY: Molecular mechanisms of long noncoding RNAs. Mol Cell 43: 904-914, 2011.
15. Tsai MC, Manor O, Wan Y, Mosammaparast N, Wang JK, Lan F, Shi Y, Segal E and Chang HY: Long noncoding RNA as modular scaffold of histone modification complexes. Science 329: 689-693, 2010.
16. Qu L, Ding J, Chen C, Wu ZJ, Liu B, Gao Y, Chen W, Liu F, Sun W, Li XF, *et al*: Exosome-transmitted lncARSR promotes sunitinib resistance in renal cancer by acting as a competing endogenous RNA. Cancer Cell 29: 653-668, 2016.
17. Chen G, Sun W, Hua X, Zeng W and Yang L: Long non-coding RNA FOXD2-AS1 aggravates nasopharyngeal carcinoma carcinogenesis by modulating miR-363-5p/S100A1 pathway. Gene 645: 76-84, 2018.
18. Li J, Zhao Y, Lu Y, Ritchie W, Grau G, Vadas MA and Gamble JR: The poly-cistronic miR-23-27-24 complexes target endothelial cell junctions: Differential functional and molecular effects of miR-23a and miR-23b. Mol Ther Nucleic Acids 5: e354, 2016.
19. Li CY, Liang GY, Yao WZ, Sui J, Shen X, Zhang YQ, Peng H, Hong WW, Ye YC, Zhang ZY, *et al*: Integrated analysis of long non-coding RNA competing interactions reveals the potential role in progression of human gastric cancer. Int J Oncol 48: 1965-1976, 2016.
20. Rong L, Zhao R and Lu J: Highly expressed long non-coding RNA FOXD2-AS1 promotes non-small cell lung cancer progression via Wnt/β-catenin signaling. Biochem Biophys Res Commun 484: 586-591, 2017.
21. Bao J, Zhou C, Zhang J, Mo J, Ye Q, He J and Diao J: Upregulation of the long noncoding RNA FOXD2-AS1 predicts poor prognosis in esophageal squamous cell carcinoma. Cancer Biomark 21: 527-533, 2018.
22. Shang W, Tang Z, Gao Y, Qi H, Su X, Zhang Y and Yang R: lncRNA RNCR3 promotes Chop expression by sponging miR-185-5p during MDSC differentiation. Oncotarget 8: 111754-111769, 2017.
23. An Q, Zhou L and Xu N: Long noncoding RNA FOXD2-AS1 accelerates the gemcitabine-resistance of bladder cancer by sponging miR-143. Biomed Pharmacother 103: 415-420, 2018.
24. Kalli S, Semine A, Cohen S, Naber SP, Makim SS and Bahl M: American Joint Committee on Cancer's Staging System for Breast Cancer, Eighth Edition: What the radiologist needs to know. Radiographics 38: 1921-1933, 2018.
25. Livak KJ and Schmittgen TD: Analysis of relative gene expression data using real-time quantitative PCR and the 2(-Δ Δ C(T)) Method. Methods 25: 402-408, 2001.
26. Peng F, Li TT, Wang KL, Xiao GQ, Wang JH, Zhao HD, Kang ZJ, Fan WJ, Zhu LL, Li M, *et al*: H19/let-7/LIN28 reciprocal negative regulatory circuit promotes breast cancer stem cell maintenance. Cell Death Dis 8: e2569, 2017.
27. Cai Z and Liu Q: Cell Cycle regulation in treatment of breast cancer. Adv Exp Med Biol 1026: 251-270, 2017.
28. Wang T: Association between HIF1α 1772 C/T polymorphism and breast cancer susceptibility: A systematic review. Crit Rev Eukaryot Gene Expr 27: 297-304, 2017.
29. Wang J and Sun G: FOXO1-MALAT1-miR-26a-5p feedback loop mediates proliferation and migration in osteosarcoma cells. Oncol Res 25: 1517-1527, 2017.
30. Liu Y, Choi DS, Sheng J, Ensor JE, Liang DH, Rodriguez-Aguayo C, Polley A, Benz S, Elemento O, Verma A, *et al*: HN1L promotes triple-negative breast cancer stem cells through LEPR-STAT3 pathway. Stem Cell Reports 10: 212-227, 2018.
31. Safa AR: Resistance to cell death and its modulation in cancer stem cells. Crit Rev Oncog 21: 203-219, 2016.
32. Gao YL, Zhao ZS, Zhang MY, Han LJ, Dong YJ and Xu B: Long noncoding RNA PVT1 facilitates cervical cancer progression via negative regulating of miR-424. Oncol Res 25: 1391-1398, 2017.
33. Koshizuka K, Hanazawa T, Kikkawa N, Katada K, Okato A, Arai T, Idichi T, Osako Y, Okamoto Y and Seki N: Antitumor miR-150-5p and miR-150-3p inhibit cancer cell aggressiveness by targeting SPOCK1 in head and neck squamous cell carcinoma. Auris Nasus Larynx 45: 854-865, 2018.
34. Cui XB, Zhang SM, Xu YX, Dang HW, Liu CX, Wang LH, Yang L, Hu JM, Liang WH, Jiang JF, *et al*: PFN2, a novel marker of unfavorable prognosis, is a potential therapeutic target involved in esophageal squamous cell carcinoma. J Transl Med 14: 137, 2016.
35. Kim MJ, Lee YS, Han GY, Lee HN, Ahn C and Kim CW: Profilin 2 promotes migration, invasion, and stemness of HT29 human colorectal cancer stem cells. Biosci Biotechnol Biochem 79: 1438-1446, 2015.